Carbohydrate Polymers 92 (2013) 260–268

Contents lists available at SciVerse ScienceDirect

Carbohydrate Polymers

journal homepage: www.elsevier.com/locate/carbpol

Preparation of starch-stabilized silver nanoparticles from amylose–sodium palmitate inclusion complexes☆

George F. Fanta[a], James A. Kenar[b,*], Frederick C. Felker[b], Jeffrey A. Byars[b]

[a] Plant Polymer, National Center for Agricultural Utilization Research, USDA/ARS, 1815 N. University St., Peoria, IL 61604, United States
[b] Functional Foods Research Units, National Center for Agricultural Utilization Research, USDA/ARS, 1815 N. University St., Peoria, IL 61604, United States

ARTICLE INFO

Article history:
Received 10 July 2012
Received in revised form 7 September 2012
Accepted 10 September 2012
Available online 16 September 2012

Keywords:
Silver nanoparticles
Amylose inclusion complex
Starch
Sodium palmitate
Jet-cooking

ABSTRACT

Starch-stabilized silver nanoparticles (AgNP) were prepared from amylose–sodium palmitate helical inclusion complexes by first converting sodium palmitate within the amylose helix to silver palmitate by an ion-exchange reaction with silver nitrate, and then reducing the complexed silver palmitate salt with $NaBH_4$. This process yielded stable aqueous solutions that could be dried and then re-dispersed in water for end-use applications. Reaction products were characterized by inductively coupled plasma-atomic emission spectroscopy (ICP-AES), UV–VIS spectroscopy, X-ray diffraction, TEM, SEM and light microscopy. Addition of acid to reduce the pH of aqueous starch-AgNP solutions produced an increase in viscosity, and nearly quantitative precipitation of starch-AgNP was observed at low pH. Smaller AgNP and higher conversions of silver nitrate to water-soluble starch-AgNP were obtained in this process, as compared with a process carried out under similar conditions using a commercial soluble starch as a stabilizer.

Published by Elsevier Ltd.

1. Introduction

Silver nanoparticles (AgNP) have been the subject of numerous studies, and a number of practical applications have been suggested for these materials. The antibacterial properties of AgNP are of major interest, and methods for their synthesis as well as their antimicrobial properties have been reviewed (Sharma, Yngard, & Lin, 2009). AgNP have been prepared from silver nitrate using starches or starch derivatives as stabilizers or protecting agents to retard the aggregation of AgNP, and sodium borohydride ($NaBH_4$) is frequently used to reduce silver ion to AgNP. The mechanism and by-products of this reduction process have been described (Bromberg, Chen, Chang, Wang, & Hatton, 2010). Božanić et al. (2007, 2011) used $NaBH_4$ to reduce silver nitrate using sago starch as the protecting agent; and films of sago starch with AgNP were prepared and their antimicrobial properties were examined. AgNP were also prepared inside starch-based hydrogels obtained by dissolving N-vinyl pyrrolidone, acrylamide or acrylic acid in aqueous dispersions of starch and then polymerizing the monomers using gamma irradiation (Eid, 2011). Silver nitrate solution was allowed to diffuse into the water-swollen hydrogels, and the silver ion was subsequently reduced to AgNP with $NaBH_4$. Vimala, Sivudu, Mohan, Sreedhar, and Raju (2009) also prepared hydrogels by polymerizing acrylamide in the presence of starch and a crosslinking agent. The hydrogels were then equilibrated with aqueous silver nitrate, and the entrapped silver ions were reduced with $NaBH_4$.

To avoid the use of $NaBH_4$ and the accompanying evolution of hydrogen, reducing sugars such as glucose have also been used as reducing agents for silver ion, and the mechanism for this reduction process has been described (Batabyal, Basu, Das, & Sanyal, 2007). Raveendran, Fu, and Wallen (2003) and Raveendran, Fu, and Wallen (2006) added silver nitrate solution to aqueous solutions of soluble starch and carried out the reduction by adding glucose and then heating the resulting dispersions. Shervani and Yamamoto (2011) also reduced silver nitrate with β-D-glucose in an aqueous gel of soluble starch. A U.S. patent application (Islam, 2010) describes the use of microwave heating to reduce silver ion to AgNP using carbohydrates such as glucose, sucrose, fructose, galactose, ribose and lactose as reducing agents. Valodkar, Bhadoria, Pohnerkar, Mohan, and Thakore (2010) also prepared AgNP by adding aqueous solutions of sucrose, soluble starch and waxy corn starch to aqueous solutions of silver nitrate and then heating the solutions in a microwave oven. Gao, Wei, Yan, and Xu (2011) prepared AgNP using soluble starch as the stabilizer and glucose as the reducing agent, and the interplanar crystal spacing in the resulting AgNP was determined. Starch and glucose reducing agent were similarly

☆ Names are necessary to report factually on available data; however, the USDA neither guarantees nor warrants the standard of the product, and use of the name by USDA implies no approval of the product to the exclusion of other that may also be suitable.

* Corresponding author. Tel.: +1 309 681 6360; fax: +1 309 681 6685.
E-mail address: jim.kenar@ars.usda.gov (J.A. Kenar).

0144-8617/$ – see front matter. Published by Elsevier Ltd.
http://dx.doi.org/10.1016/j.carbpol.2012.09.016

used by Luo, Chen, Chen, Xu, and Zhang (2012) to prepare AgNP, and their antibacterial properties in polyethylene packaging film was determined.

AgNP were also prepared using soluble starch as both the stabilizing agent and reducing agent (Vigneshwaran, Nachane, Balasubramanya, & Varadarajan, 2006). Elevated temperatures were obtained by heating in an autoclave, where hydrolysis of starch can take place to form sugars and dextrins having reducing end groups. Silver sulfate was also used as a source of AgNP, and these reactions were similarly carried out in an autoclave at 160 °C (Valodkar et al., 2010). The reduction of silver nitrate in an aqueous solution of soluble starch was also carried out by irradiating the solution with Co^{60} (Kassaee, Akhavan, Sheikh, & Beteshobabrud, 2008). A mesoporous starch gel was also used as a stabilizer, support and reducing surface for the preparation of AgNP with antimicrobial properties (White, Budarin, Moir, & Clark, 2011). El-Rafie et al. prepared AgNP from silver nitrate using aqueous alkaline solutions of hydroxypropyl starch as the stabilizing and reducing agent (El-Rafie et al., 2011), and AgNP solutions were then applied to cotton fabrics to impart antimicrobial properties (Hebeish et al., 2011).

Reducing agents other than $NaBH_4$ and carbohydrates have also been used to prepare starch-stabilized AgNP. Valodkar, Modi, Pal, and Thakore (2011) used ascorbic acid and microwave heating to reduce silver nitrate to AgNP in aqueous solutions of starch; and Hu and coworkers (Hu, Wang, Wang, Zhang, & Yu, 2008) used microwave heating to prepare starch-stabilized AgNP using basic amino acids as reducing agents. *Mesua ferrea* L. aqueous leaf extract was examined as a reducing agent in the presence of soluble starch (Konwarh, Karak, Sawian, Baruah, & Mandal, 2011), and a mixture of soluble starch and the supernatant of a fungal culture was also used (Ghaseminezhad, Hamedi, & Shojaosadati, 2012). Kakkar, Sherly, Madgula, Devi, and Sreedhar (2012) prepared AgNP using combinations of starch and trisodium citrate as reducing and stabilizing agents.

In the present study, starch-stabilized AgNP were prepared from amylose–sodium palmitate inclusion complexes (Am–Na Palm) by first ion exchanging sodium palmitate within the amylose helix with silver nitrate to obtain the silver palmitate salt, and then reducing silver ion to AgNP with $NaBH_4$. Although various starches and starch derivatives have been used as stabilizers and delivery agents for AgNP, the use of amylose inclusion complexes for this purpose has not been reported. The inclusion complex used in this study was prepared by blending a water solution of sodium palmitate with a hot, jet-cooked dispersion of high amylose corn starch (Fanta, Kenar, Byars, Felker, & Shogren, 2010). Steam jet-cooking at high temperatures and pressures has been used by the starch industry for decades as a rapid, inexpensive and continuous method for preparing starch solutions and dispersions (Klem & Brogley, 1981). Physical modification by steam jet-cooking and complex formation is a viable alternative to chemical modifications of starch with acids or other chemical reagents to increase water solubility and improve the functionality of starch as a stabilizing agent for AgNP. Industrially, starch has been made more water soluble through the Lintner procedure by treating granular starch with acid for time periods ranging from days to weeks (Johnston, Mukerjea, & Robyt, 2011; Lintner, 1886; Ma & Robyt, 1987). This process is still in commercial use today to produce products referred to as soluble starch. These products however are only marginally water soluble (Johnston et al., 2011; Ma & Robyt, 1987). Although they can be gelatinized and dispersed in water at lower temperatures than native unmodified starch, a significant percentage of the dispersed starch remains as an insoluble gel, and a major portion of the AgNP produced from these materials, therefore, remains associated with the insoluble portion of the final product. In contrast, Am–Na Palm prepared by our jet-cooking process is water soluble because the retrogradation of amylose is inhibited by the water-solubility of complexed sodium palmitate and also the charge repulsion between amylose macromolecules due to the ionic nature sodium palmitate within the amylose helix (Byars, Fanta, Kenar, & Felker, 2012; Fanta et al., 2010). Increases in the viscosity of Am–Na Palm solutions and the formation of gel were observed when acid was added to reduce the pH from its initial value of 8 to 5.0–5.5. Further reduction of the pH to 3.6 caused the amylose complex to precipitate from solution due to conversion of complexed sodium palmitate to water insoluble palmitic acid. In this study we will show that similar properties are exhibited by the starch-stabilized AgNP prepared from these amylose complexes. The ability to prepare aqueous AgNP containing gels and to precipitate starch-stabilized AgNP onto various substrates by a simple adjustment in pH are properties that could have commercial utility. Also, these AgNP preparations can be dried and then re-dissolved in water at a later time when needed. Although reduction with $NaBH_4$ is not an environmentally friendly process, this reducing agent was used in this study because it was necessary to confirm the functionality of Am–Na Palm as a stabilizer for AgNP under conditions that have been proven to rapidly and quantitatively reduce silver ion to AgNP. Preliminary experiments with glucose as the reducing agent suggest that more environmentally friendly reducing agents can be used as an alternative in our system.

2. Materials and methods

2.1. Materials

High-amylose corn starch, containing approximately 70% apparent amylose, was AmyloGel 03003 from Cargill Inc., Minneapolis, MN. Soluble starch (ASC reagent) was purchased from Sigma–Aldrich. Percent moisture in starch samples was determined by weight loss after drying for 4 h at 100 °C over P_2O_5 under vacuum, and all weights of starch-based products are given on a dry-weight basis. Sodium palmitate (98.5%) was purchased from Sigma, St. Louis, MO. Silver nitrate (99+%) and sodium borohydride (≥98.5%) were purchased from Sigma–Aldrich, St. Louis, MO.

2.2. Preparation of amylose–sodium palmitate complex (Am–Na Palm)

The procedure used was similar to that reported in an earlier study (Fanta et al., 2010). High-amylose corn starch (150.0 g) was dispersed in 2700 mL of water, and the slurry was passed though a Penick and Ford (Penford Corp., Englewood, CO) laboratory model steam jet-cooker operating under excess-steam conditions (Klem & Brogley, 1981). Temperature in the hydroheater was 140 °C, the steam back pressure was 380 kPa (40 psig) and the steam line pressure from the boiler was 550 kPa (65 psig). Pumping rate through the jet-cooker was 1 L/min. The hot, jet-cooked starch dispersion was collected in a Waring stainless steel blending container (Waring Products Division, New Hartford, CT) that was previously heated with 100 °C water from the jet-cooker. The jet-cooker was flushed with water to maximize the amount of starch collected. The weight of jet-cooked dispersion collected in the blending container was 3370 g, and the concentration of starch in the jet-cooked dispersion was 4.32 wt%, determined by freeze-drying a weighed portion of jet-cooked dispersion. These values were then used to calculate the weight of starch collected, which was 97% of the initial weight of starch used. Quantitative recovery of the initial weight of starch was not achieved due to retention of small amounts of starch in plumbing of the jet-cooking assembly.

The weight of sodium palmitate used to form the amylose complex was 7.875 g (7.5% of the weight of apparent amylose in 150 g of

starch). Sodium palmitate was dissolved in 300 mL of water at 94 °C, and the resulting clear solution was added to the hot starch dispersion immediately after it was collected from the jet-cooker. The hot dispersion was slowly stirred for 2 min, and was then transferred to a 4-L beaker and cooled in an ice-water bath to 25 °C. The cooled solution was centrifuged (Beckman J2-21 ME centrifuge (Palo Alto, CA) equipped with a JA-10 rotor rotating at 10,000 rpm and an RCF (relative centrifugal force) of approximately 17,648 × *g*) to remove a small amount of insoluble solid (less than 1% of the starting weight of starch). The centrifuged solution was then freeze-dried. Since only 97% of the initial weight of starch was recovered in the jet-cooked dispersion, the actual percentage of sodium palmitate in the freeze-dried product was 7.76%, based on apparent amylose.

2.3. Preparation of starch-stabilized AgNP from freeze-dried Am–Na Palm

Freeze-dried Am–Na Palm (1.00 g) was dispersed in 100 g of water in a 150 mL beaker, and the dispersion was stirred with a magnetic stir-bar and heated on a temperature-controlled stirring hot plate to 80 °C. The hot plate was a Model IKA RCT Basic S1 supplied by IKA-Works (Wilmington, NC) and was controlled with an IKA ETS-D4 Fuzzy Temperature Controller from the same company. A clear solution was obtained at 80 °C. The ion exchange reaction with silver nitrate was carried out at 80 °C by using a microliter syringe to add measured volumes of a solution of 1.00 g of silver nitrate in 10.0 mL of water. The resulting mixtures were then stirred at 80 °C for 45 min. The volumes of silver nitrate solution used were calculated to convert either 75% (235 μL) or 30% (94 μL) of the complexed sodium palmitate to the silver salt. The clear Am–Na Palm solutions became turbid when silver nitrate solution was added at the 75% level; however only slight turbidity was observed at the 30% level. $NaBH_4$ solutions were prepared immediately before use by dissolving 0.523 g of $NaBH_4$ in 10 mL of water at room temperature, and the solutions were added at 80 °C. The volumes of $NaBH_4$ solution added to the Am–Na Palm/silver nitrate dispersions were calculated to provide either a 1.25-fold excess, a 2.5-fold excess or a 3.12-fold excess over the amount theoretically needed for the reduction. The dispersions turned dark brown immediately after addition, and foaming was observed due to evolution of hydrogen. The dispersions were removed from the hot plate and allowed to stir and cool to room temperature under ambient conditions for 4 h. The cooled dispersions were then centrifuged on an IEC HT centrifuge (International Equipment Co. Inc., Chattanooga, TN) at 9500 rpm (10,494 × g) for 45 min, and the insoluble solids were washed twice by re-suspending in water followed by centrifugation. The insoluble solids were dried in tared aluminum pans for 16 h at 70 °C, and the weights of dry solids were determined. The clear, orange supernatant solutions (plus washings) obtained by centrifugation were freeze-dried to determine percent solids, after removal of small amounts for UV–VIS spectroscopy, transmission electron microscopy (TEM), and analysis for silver by inductively coupled plasma-atomic emission spectroscopy (ICP-AES).

2.4. Inductively coupled plasma-atomic emission spectroscopy (ICP-AES) analysis for silver

ICP-AES analyses to determine ppm silver were carried out on the clear supernatants obtained after removal of insoluble solids by centrifugation. Percent solids in these solutions were determined by freeze-drying weighed amounts of solution. ICP-AES was performed using a Perkin Elmer 7000DV ICP (Shelton, CT) instrument optimized at 328.068 nm on aqueous solutions of known solids percentages to quantify the amounts of silver contained in the samples. Samples were analyzed axially to establish a lower limit of detection (effectively less than 0.1 ppm). A three-point calibration at 1.00, 5.00 and 10.00 ppm was prepared from an external 1000 ppm standard silver solution (Spex CertiPrep Cat #CLAG2-2Y Lot #CL4-132AG) by appropriate dilution. A 7.5 ppm verification sample was made independently and was tested before and after all samples. A new calibration curve was created for each set of data that was produced. The percentage of initially added silver (added as silver nitrate) that was converted to water-soluble starch-AgNP by our reaction process was then calculated from the weight of silver nitrate used in the ion-exchange reaction and the ppm concentration of silver and wt% solids in the solution analyzed by ICP-AES.

2.5. UV–VIS

Ultraviolet–visible (UV–VIS) absorption spectra were obtained at concentrations of 0.3% total solids on a Shimadzu UV 1601UV spectrophotometer (Duisburg, F.R. Germany), scanning from 190 to 900 nm. Samples were diluted with Millipore-filtered deionized water and were run in disposable 1.5 mL plastic cuvettes (Fisher, Style no.: 14955127). Millipore-filtered deionized water was used in the reference cell.

2.6. X-ray diffraction

Freeze-dried samples were equilibrated at 23 °C and 45% relative humidity prior to analysis. X-ray powder diffraction patterns were obtained with a Phillips 1820 diffractometer (Philips Electronic Instruments Co., Mahwah, NJ) operated at 40 kV with a graphite-filtered Cu K_α radiation and a θ compensating slit. Data were acquired in $2\theta = 0.05°$, 4 s steps.

2.7. Preparation of starch-AgNP dispersions for rheological measurements

The product used for these experiments was the freeze-dried, water-soluble fraction obtained in Experiment 1, Table 1 ($AgNO_3$: 75% of theoretical; $NaBH_4$: 2.5-fold molar excess). To remove water-soluble inorganic salts, 0.8 g of freeze-dried sample was dissolved in 35 mL of water at 80 °C, and the resulting cooled solution was dialyzed at room temperature against deionized water. Dialysis was carried out in 2 L of deionized water for 44 h with three changes of water during this time period. The dialysis membrane was Spectra/Por® Molecularporous Membrane, MWCO: 6–8000, flat width: 50 mm (Spectrum Medical Industries Inc., Los Angeles, CA). The dialyzed solution was freeze-dried.

Solutions for rheological measurements were prepared by dispersing 0.200 g of dialyzed, freeze-dried sample in 9.8 g of water in 20 mL scintillation vials. The dispersions were stirred and heated to 80 °C to dissolve the sample, and varying amounts of 0.1 M acetic acid (80, 94, and 140 μL) were added to lower the pH to 6.40, 6.17, and 5.75, respectively. The samples were stirred for 10 min at 80 °C and were then removed from the heat and allowed to cool without stirring to 25 °C. The pH of cooled dispersions was measured with an Orion 8235BN electrode and a ThermoOrion pH meter (Thermo Fisher Scientific, Waltham, MA).

The concentration of silver (ppm) remaining in the water solutions after acidifying to pH 5.75 and 3.94 was determined by ICP-AES, after removing the insoluble, AgNP-containing precipitate by centrifugation at 14,000 rpm (16,000 × *g*) using an Eppendorf microcentrifuge, Model 5451 C (Engelsdorf, Germany). For the determination carried out at pH 3.94, 7 g of the dispersion previously prepared at pH 6.40 was further acidified by adding 100 μL of 1 M acetic acid. The dispersion was then centrifuged as described above, and the clear supernatant was analyzed for silver by ICP-AES. The acid-precipitated solid separated by centrifugation was washed by dispersing in water and centrifuging as described above. The water-washed solid was then dispersed in water, 100 μL of the

Table 1
Preparation of starch-based AgNP. Amylose–sodium palmitate complex (Am–Na Palm) versus soluble starch.

Experiment	Starch material used	$AgNO_3$ added		$NaBH_4$ used		Water-soluble fraction			
		10% solution (μL)	% of theory[a]	5.23% solution (μL)	X-fold molar excess	pH	% of total weight[b]	Ag content (wt%)[c]	% of added Ag in soluble fraction
1	Am–Na Palm	235	75	250	2.5	8.66	98.5	0.46	32.5
2	Am–Na Palm	235	75	125	1.25	7.86	98.5	0.47	33.1
3	Am–Na Palm	94	30	125	3.12	8.57	99.9	0.49	86.4
4	Soluble starch	94	–	125	3.12	8.50	20.0	1.42	49.3

[a] Percent of the theoretical amount of $AgNO_3$ solution needed to ion-exchange all of the Na^+ in the Am–Na Palm complex.
[b] Percent of the total weight of dry product (soluble + insoluble).
[c] Percent Ag by weight in the dry water soluble product.

dispersion was added to 20 mL of absolute ethanol, and the solid particles were allowed to settle. The settled solid was washed with fresh ethanol by re-suspending and settling, and the ethanol-wet precipitate was critical-point dried with CO_2 onto aluminum stubs for SEM.

2.8. Rheological property measurements

Measurements in small amplitude oscillatory shear flow were conducted on an ARES LS1 controlled strain fluids rheometer (TA Instruments, New Castle, DE). Tests were performed with a 50 mm diameter parallel plate geometry at strains within the linear viscoelastic region for all samples. A Peltier plate was used to maintain the temperature at $25.0 \pm 0.1\,^{\circ}C$. Sample edges were coated with mineral oil, and humidity covers were used to prevent drying of the samples.

2.9. Microscopy

2.9.1. Light microscopy

Particles were observed with a Zeiss Axioskop light microscope equipped with an AxioCam ICc 3 digital camera (Carl Zeiss Inc., Thornwood, NY) using phase-contrast optics.

2.9.2. Scanning electron microscopy (SEM)

Samples were critical-point dried with CO_2 onto aluminum stubs, and the dried specimens were sputter-coated with Au–Pd and examined and photographed with a JEOL 6400 V scanning electron microscope (JEOL, USA, Peabody, MA).

2.9.3. Transmission electron microscopy (TEM)

Silver nanoparticle fractions were diluted 1:10 or 1:100 with water. Diluted samples (1 μL) were applied directly to carbon films on 200-mesh copper grids and allowed to air dry. Specimens were examined with a JEOL 2100 LaB_6Cryo TEM operating at 200 kV. Images were obtained with a Gatan UltraScan 2kx2k CCD camera (Gatan Inc., Pleasanton, CA). Particle size distributions were obtained by analyzing electron micrographs after adjusting image contrast to enable threshold detection of individual particles. Particle diameters were determined using Gatan Digital Micrograph software (Gatan Inc., Pleasanton, CA). The number of particles analyzed from TEM images of the soluble fractions of Experiments 1–4 in Table 1 was 383, 1078, 498, and 4,458, respectively. Means and standard deviations were based on Gaussian curve fits obtained with Origin Pro version 7.5 software (OriginLab Corp., Northampton, MA).

3. Results and discussion

Results of reactions carried out under different experimental conditions are shown in Table 1. In Experiments 1 and 2, the amount of silver nitrate added was 75% of the amount theoretically needed to ion-exchange all of the sodium ion for silver ion in the Am–Na Palm complex. The amount of silver nitrate used was less than theoretical to minimize the amount of silver ion that remained unassociated with the amylose complex. In Experiment 1, the amount of $NaBH_4$ used was 2.5 times the theoretical amount needed for complete reduction, whereas a 1.25-fold excess of $NaBH_4$ was used in Experiment 2. Although the pH of the final dispersion after reduction was higher in Experiment 1, due to the larger amount of $NaBH_4$ used, similar products were obtained in these two experiments, and the amounts of originally added silver ion that were converted to water-soluble starch-AgNP were also similar (32.5% vs. 33.1%). The low conversions of silver ion to water-soluble starch-AgNP indicate that most of the added silver was converted to water-insoluble products, and was now part of the dark-brown, water-insoluble material removed by centrifugation. In experiments 1 and 2, this insoluble material amounted to 1.5 wt% of the total product.

Since water solubility of starch-AgNP is a desirable property for many practical applications, we considered methods for increasing the percent conversion of added silver nitrate to water-soluble starch-AgNP, and thus improve the efficiency of our process with respect to utilization of the expensive silver component. Experiment 3 (Table 1) shows that one method for accomplishing this goal is to simply reduce the amount of silver nitrate used in the ion-exchange reaction. When the amount of silver nitrate was reduced from 75% to 30% of the amount theoretically needed for the ion exchange, the insoluble fraction remaining after centrifugation was reduced from 1.5 wt% to 0.1 wt% of the total isolated solid, and the percentage of added silver that was incorporated into the water-soluble fraction was increased to 86.4%. These results are consistent with our observation that addition of silver nitrate at the 75% level to a clear solution of amylose–sodium palmitate complex at 80 °C increased the turbidity of the dispersion, probably due to the reduced solubility of silver palmitate relative to sodium palmitate in the amylose complex. Once the amylose complex is precipitated from water solution, re-dissolving the complex can be difficult due to association and hydrogen-bonding between hydroxyl groups, analogous to the retrogradation process that takes place in aqueous solutions of amylose. In contrast, only a slight increase in turbidity, and thus less precipitation of insoluble complex, was observed when silver nitrate was added at the 30% level. Although a detailed study of the storage stability of these starch-AgNP solutions has not yet been carried out, it was observed that the water-soluble fraction obtained in Experiment 3 (with solids content of 0.9%) remained clear and contained no precipitated solid after standing for 30 days at ambient room temperature. According to the published mechanism for the reduction of silver ion with $NaBH_4$ (Bromberg et al., 2010), the sodium salt of complexed palmitic acid is re-formed as the silver ion is reduced to AgNP. In the case of Am–Na Palm, the silver palmitate obtained through ion exchange with silver nitrate produces AgNP upon $NaBH_4$ reduction and reforms the Am–Na Palm complex, thus enhancing the water solubility of the final starch-AgNP products. Consistent with

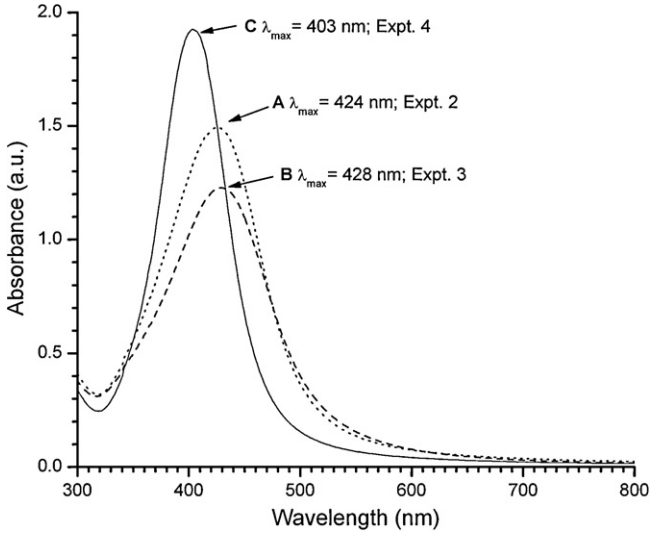

Fig. 1. UV–VIS spectra of water soluble AgNP fractions at solids concentration of 0.3 wt%. (A) Water-soluble fraction isolated in Experiment 2, Table 1; (B) Water-soluble fraction isolated in Experiment 3, Table 1; (C) Water-soluble fraction isolated in Experiment 4, Table 1 (commercial soluble starch used as stabilizer).

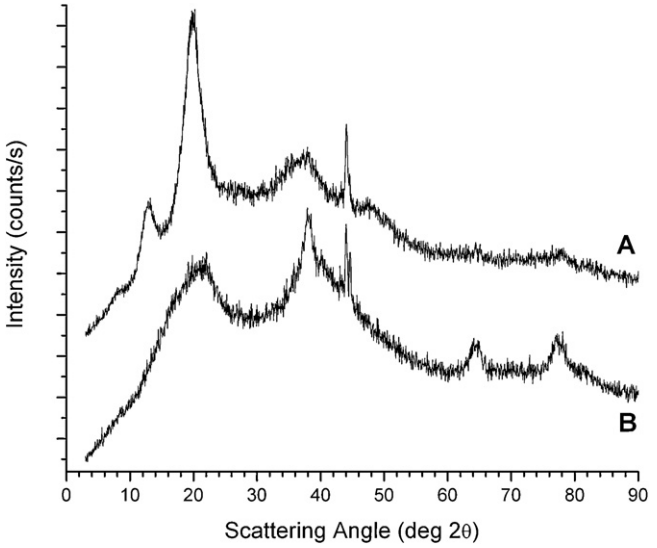

Fig. 2. X-ray diffraction patterns of freeze-dried samples of the water-soluble fractions isolated in: (A) Experiment 3, Table 1 (Am–Na Palm complex); (B) Experiment 4, Table 1 (commercial soluble starch used as stabilizer).

this mechanism, our reaction products exhibited a high level of water-solubility, and only minor amounts of insoluble material were removed by centrifugation.

Since commercial starches have been frequently used as stabilizers in the preparation of aqueous AgNP dispersions, Experiment 4, Table 1 was carried out with a commercial sample of soluble starch (not jet cooked) under the same conditions and with the same weights of starch, silver nitrate and $NaBH_4$ used in Experiment 3. In contrast to Experiment 3, the water-soluble fraction obtained with soluble starch amounted to only 20% of the total isolated solid (80% precipitated as a swollen solid after centrifugation), and only 49.3% of the added silver was incorporated into the water-soluble fraction.

As noted earlier, the water-soluble fractions obtained by $NaBH_4$ reduction were deep orange in color, indicative of AgNP. UV–VIS spectroscopy is commonly used to observe the surface plasmon resonance bands of metal nanoparticles. Plasmonic properties are a characteristic optical property of metal nanoparticles and are highly dependent on the size, shape and dielectric properties of the nanoparticle and the adherence of stabilizers to the nanoparticle surface. Accordingly, the UV–VIS spectra in Fig. 1 showed strong surface plasmon resonance band maxima at 403, 424, and 428 nm, respectively, for the water-soluble fractions isolated in Experiments 4, 2, and 3 of Table 1. Spectra were all obtained at a total solids concentration of 0.3%. The spectrum of the water-soluble fraction from Experiment 1 is not shown, since the values for λ_{max} and absorbance of the surface plasmon resonance band for this material (λ_{max} = 424 nm; absorbance = 1.57) were similar to those observed for the soluble fraction isolated from Experiment 2 (λ_{max} = 424 nm; absorbance = 1.49 in Fig. 1A). Although λ_{max} for the soluble fraction obtained from Experiment 3 (Fig. 1B, λ_{max} = 428 nm) was similar to that observed for the soluble fraction in Experiment 2, a lower absorbance value was observed. A λ_{max} value of 403 nm (Fig. 1C) was observed for the water-soluble fraction obtained from the soluble starch experiment (Experiment 4); and a higher absorbance value was observed for this fraction, consistent with the higher percentage of silver in the relatively low percentage of water-soluble material isolated (20% of total weight). The λ_{max} value of 403 nm was similar to that observed by Hu et al. (2008).

Fig. 2A shows the X-ray diffraction pattern of a freeze-dried sample of the water-soluble fraction isolated in Experiment 3, Table 1. The reflections at 12.7 and 20.1° 2θ are indicative of a 6_1V amylose helical complex and match the reflections previously observed for a Am–Na Palm complex prepared from high-amylose corn starch (Fanta et al., 2010). Reflections for silver nanoparticles within the starch matrix were also observed at 37.5, 44.0, 64.7 and 77.9° 2θ. Similar reflections have been observed for starch-stabilized AgNP (Eid, 2011; Gao et al., 2011; Valodkar et al., 2010; Vigneshwaran et al., 2006) and these reflections have been assigned to the (1 1 1), (2 0 0), (2 2 0) and (3 1 1) planes, respectively, of the face-centered cubic structure of silver. The most intense reflection for AgNP in Fig. 2A was at 44.0° 2θ, whereas the other three were less prominent due to the low concentration of silver in the freeze-dried sample (0.49%). Fig. 2B shows an X-ray diffraction pattern of the freeze-dried water-soluble fraction obtained from soluble starch (Experiment 4, Table 1). As expected, the diffraction pattern did not contain the 6_1V reflections characteristic of an amylose inclusion complex; however, reflections due to AgNP were observed at scattering angles similar to those shown in Fig. 2A. The intensities of the (1 1 1), (2 2 0) and (3 1 1) reflections in Fig. 2B were greater than those observed in Fig. 2A due to the higher concentration of silver in the sample (1.42%).

Typical TEM fields for AgNP obtained with amylose–sodium complexes and with the commercial sample of soluble starch are shown in Fig. 3A and B, respectively. In both cases, particles appeared spherical and well-separated, however the particles obtained with soluble starch were both larger overall and more heterogeneous in diameter (Fig. 3B, which is one fifth the magnification of Fig. 3A). Many of the nanoparticles were deposited on the substrate film at an angle that revealed the parallel lattice fringe pattern commonly associated with AgNP (Fig. 4A). The distance between the crystal planes was 0.223 nm, which is consistent with the established value for bulk silver crystals (Gao et al., 2011). Dispersions of the insoluble solids separated by centrifugation were also examined, and were found to contain, in addition to AgNP in the same size range as the supernatants, much larger aggregates. These ranged from relatively loose aggregates (Fig. 4B) with spaces between the individual particles to large, dense aggregates appearing more tightly packed (Fig. 4C). Occasionally a coating layer was observed on the larger, denser aggregates (arrows, Fig. 4C). These coatings, as well as the spaces between particles in the loose aggregates, suggest that the starch component

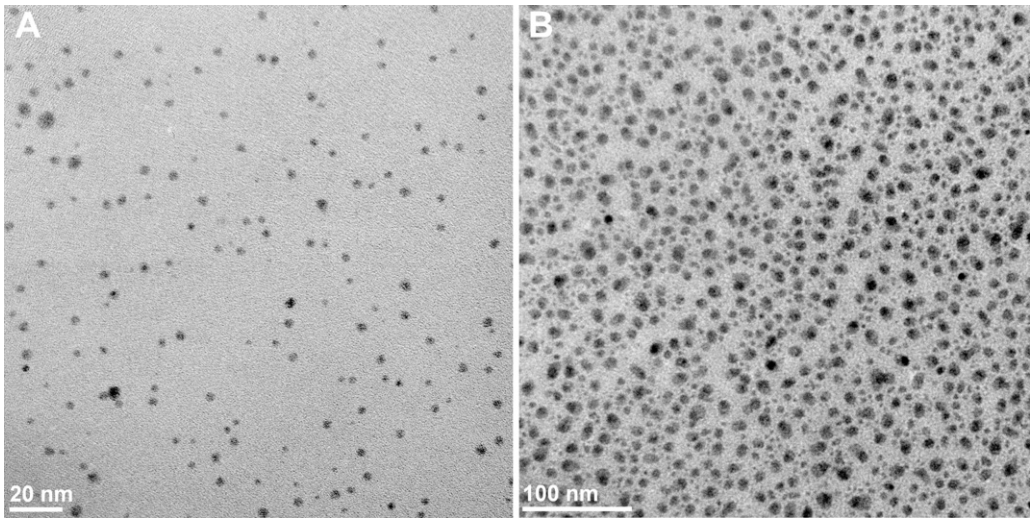

Fig. 3. Transmission electron micrographs of water soluble AgNP fractions prepared from: (A) Am–Na Palm (Experiment 3, Table 1) and (B) commercial soluble starch (Experiment 4, Table 1).

of the dispersions plays a role in stabilizing and separating the AgNP.

The size distribution of AgNP from Experiment 1 (Fig. 5A) was essentially Gaussian with a mean particle diameter of 5.24 nm (SD = 1.32 nm). Experiments 2 and 3 (Fig. 5B and C) yielded slightly smaller particles with narrower distributions. Mean particle diameters in Fig. 5B and C were 3.20 nm (SD = 0.66 nm) and 3.65 nm (SD = 0.74 nm), respectively. Since Experiments 1 and 2 were performed with the same (higher) $AgNO_3$ level while Experiments 2 and 3 were performed with the same (lower) $NaBH_4$ concentration in water, it would appear that the reductant level had a greater influence than the silver content in determining particle size in these particular treatments, possibly due to a difference in the rate of particle formation. In contrast, the AgNP obtained in Experiment 4 with soluble starch were larger and had a bimodal distribution (Fig. 5D). Based on the valley observed in the distribution curve, two populations of particles were considered: particles <35 nm in diameter with a mean of 12.90 nm and SD of 3.20 nm, and particles 35–80 nm in diameter with a mean of 51.82 nm and SD of 10.70 nm. The much larger size of these particles is consistent with the higher percentage of silver in the dry water soluble product, and also with the observation that about half of the added silver was found in the insoluble fraction comprising 80% of the total amount of material in this preparation. A wide range of AgNP sizes has been reported in the literature among those studies in which starch was used as a stabilizing agent. In most cases, typical diameters were in the range of 8–25 nm or larger (e.g. Božanić et al., 2007, 2011; Eid, 2011; Gao et al., 2011; Ghaseminezhad et al., 2012; Hu et al., 2008; Kakkar et al., 2012; Kassaee et al., 2008; Marie Arockianathan, Sekar, Kumaran, & Sastry, 2012; Valodkar et al., 2010; Vigneshwaran et al., 2006; Vimala et al., 2009; White et al., 2011) although relatively few studies revealed particles approximately 5 nm in diameter (e.g. Raveendran et al., 2003, 2006). The smaller AgNP particle size in experiments carried out with the amylose complex, as compared with that observed with soluble starch, may be due to the fact the silver ions are ionically bound to anionic palmitate within the amylose helix prior to reduction as opposed to being more loosely adsorbed onto the starch matrix. It has been shown that smaller AgNP diameters provide better antimicrobial performance than larger ones (Morones et al., 2005; Vimala et al., 2009), which suggests that the AgNP prepared with Am–Na Palm complexes

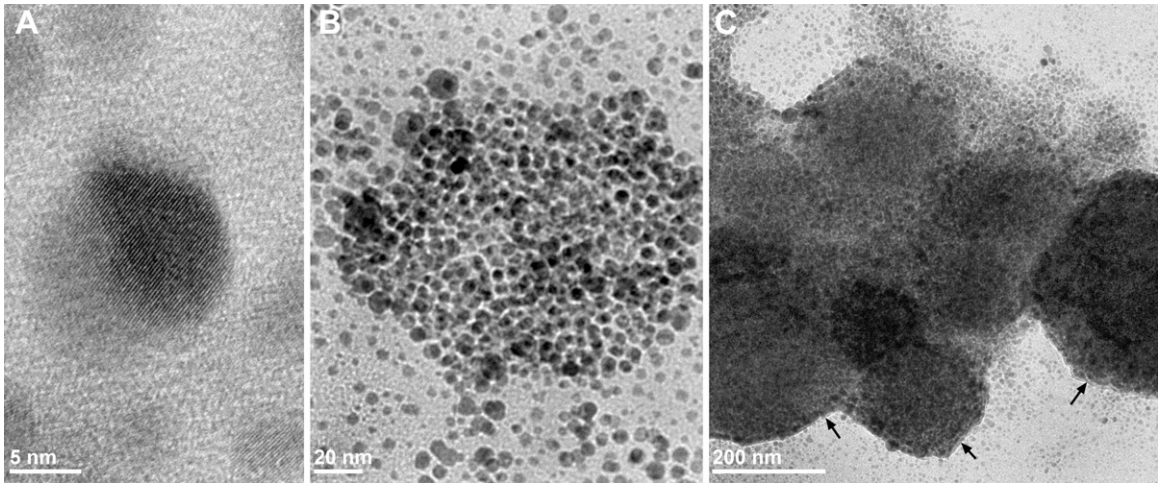

Fig. 4. Transmission electron micrographs of (A) AgNP from the soluble fraction of Experiment 3, Table 1, showing the crystal lattice structure with interplanar distance = 0.223 nm; (B) loose aggregate and (C) dense aggregate of AgNP from the insoluble solids fraction of Experiment 1, Table 1. Arrows indicate surface coating observed at the periphery of some large, dense aggregates.

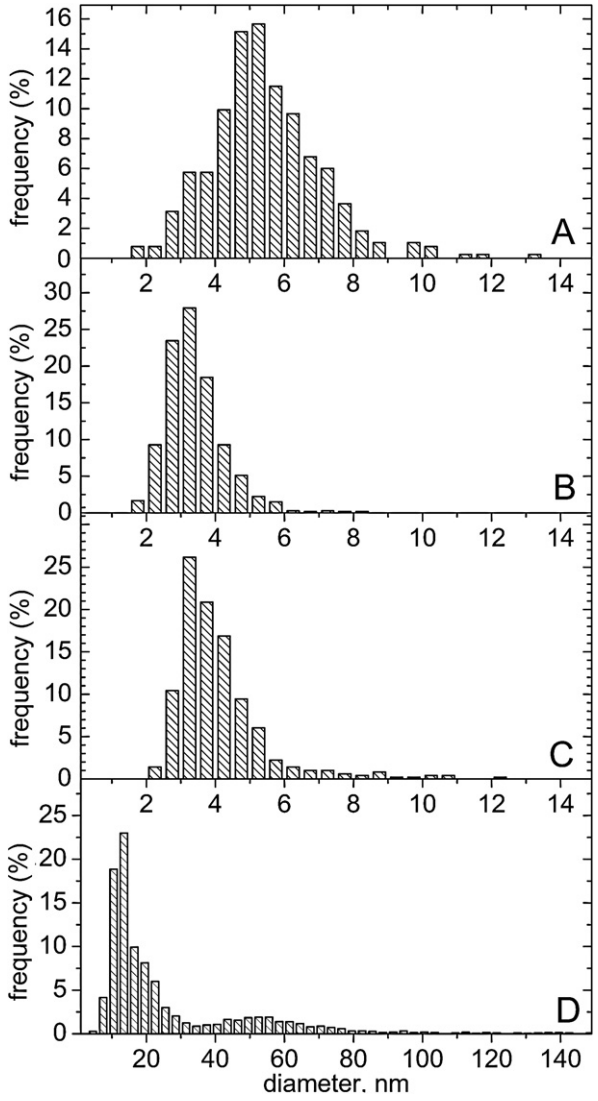

Fig. 5. Size distribution of AgNP prepared from Am–Na Palm complex in the water-soluble fractions isolated in: (A) Experiment 1, Table 1; (B) Experiment 2, Table 1; (C) Experiment 3, Table 1; and (D) Experiment 4, Table 1 (commercial soluble starch used as stabilizer).

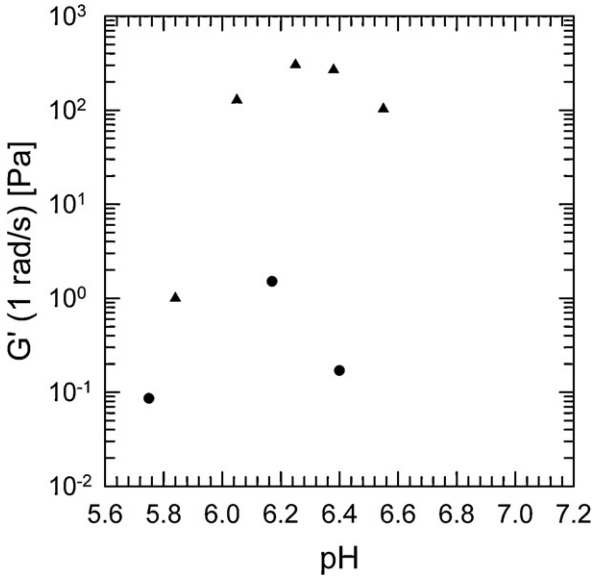

Fig. 6. Storage modulus as a function of pH for 2 wt% dispersions of: ▲ Amylose–sodium palmitate inclusion complex (Byars et al., 2012). • Water-soluble fraction isolated in Experiment 1, Table 1.

as described in this study may have an advantage with regard to antimicrobial applications.

Previously, research has shown that the rheological properties of aqueous solutions of Am–Na Palm are highly dependent on the pH of the solution (Byars et al., 2012; Fanta et al., 2010). Above pH 6.8 the complexes were water soluble and viscosities were relatively low. However, when the solutions were titrated with 0.1 M acetic acid to a pH of about 6.2, sodium palmitate within the helical complex was partially converted to water-insoluble palmitic acid. Electrostatic repulsion between amylose complexes (due to the anionic nature of the complexed sodium palmitate ligand) was therefore reduced; and junction zones were formed by hydrophobic associations between palmitic acid molecules complexed within the amylose helices, producing a gel network. The strongest gels were obtained at a pH of about 6.2. When excess acetic acid was added, complexed sodium palmitate was totally converted to palmitic acid, causing the amylose complex to precipitate from solution and producing a low-viscosity dispersion.

Experiments were carried out under similar conditions with 2% solids dispersions of the starch-AgNP product prepared in Experiment 1, Table 1. The starch-AgNP product was dialyzed to remove water-soluble inorganic salts, and 0.1 M acetic was added to reduce the pH from its initial value of 6.90–6.40, 6.17 and 5.75. Concentrations greater than 2 wt% were not examined due to the small amounts of material obtained from our small-scale experiments. Dispersions of starch-AgNP were less elastic than those prepared previously from Am–Na Palm. As indicated by the frequency-dependent storage and loss moduli and $\tan\delta > 0.4$, a viscoelastic liquid was formed from the starch-AgNP product at pH 6.17, as opposed to the gel obtained from Am–Na Palm. In Fig. 6, the storage modulus for the 2% starch-AgNP dispersion at a frequency of 1 rad/s as a function of pH is compared to the data obtained with Am–Na Palm at the same concentration (Byars et al., 2012). Although an increase in storage modulus was observed for the starch-AgNP dispersion at pH 6.17, this value was less than 1% of the maximum value of the storage modulus observed for Am–Na Palm. The lack of gel formation, the decreased values of the linear viscoelastic properties, and the narrow range of pH dependence all suggest a lower effective concentration of the complex, possibly due to the fact that complexes stabilizing the AgNP may not be available to form the gel network. Additional experiments are needed at higher concentration to completely characterize the rheological properties of these starch-AgNP materials.

As observed with water dispersions of Am–Na Palm (Byars et al., 2012; Fanta et al., 2010), lowering the pH of the starch-AgNP dispersion caused the starch-AgNP complex to precipitate from solution. ICP-AES analysis of the clear supernatant obtained by centrifugation of the dispersion acidified to pH 5.75 showed that only 0.3% of the silver initially present in the starch-AgNP sample still remained in the supernatant, indicating that essentially all of the starch-stabilized AgNP initially in solution was precipitated with the starch complex. The precipitated material was observed to consist primarily of irregularly shaped and random sized gel particles (Fig. 7A). SEM images suggested that the gel particles consisted of aggregations of small, spherical primary subunits (Fig. 7C). When excess acetic acid was added to give a pH of 3.94, the supernatant contained only 0.1% of the starch-stabilized AgNPs initially present. At this lower pH, the precipitated particles appeared more compact and denser in phase contrast micrographs (Fig. 7B), and SEM revealed aggregates of somewhat larger primary subunits (Fig. 7D). The morphologies of these precipitated particles are similar to

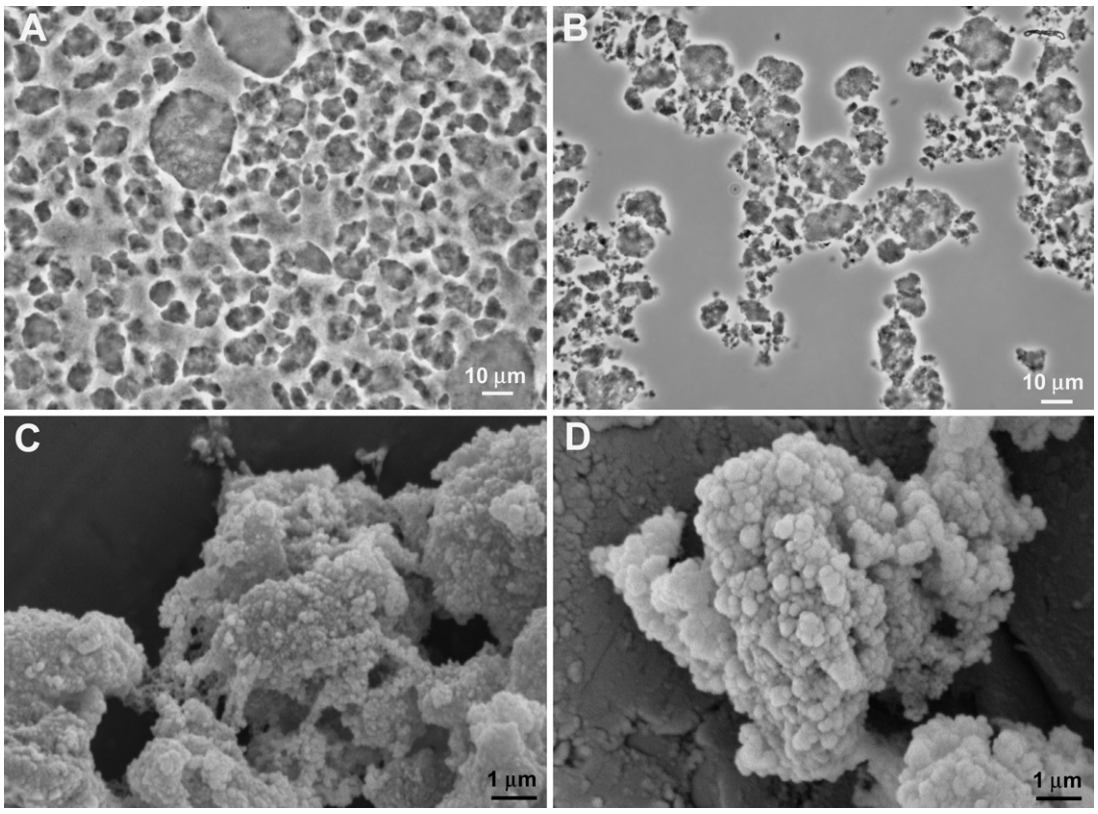

Fig. 7. Phase contrast light micrographs (A, B) and scanning electron micrographs (C, D) of precipitated particles isolated from starch-AgNP dispersions acidified to pH 5.75 (A, C) and pH 3.94 (B, D).

those previously observed for acid-precipitated samples of Am–Na Palm (Fanta et al., 2010). The AgNP contained in this material could not be seen with light microscopy or SEM, due to their small size and the fact that they are embedded in the polymer matrix of the precipitated Am–Na Palm complexes. The ability to generate AgNP in a soluble form and then render the dispersions more viscous, or precipitate the material as small gel fragments, provides a flexible approach for delivering AgNP in different applications.

4. Conclusions

Starch-stabilized silver nanoparticles were prepared from amylose–sodium palmitate helical inclusion complexes by first converting sodium palmitate within the amylose helix to silver palmitate by an ion-exchange reaction with silver nitrate, and then reducing the complexed silver salt with $NaBH_4$. This process yielded stable aqueous solutions of starch-stabilized AgNP that could be dried and then re-dispersed in water for end-use applications. The rheological properties of these aqueous solutions were highly dependent on the pH of the solution. Addition of dilute acetic acid produced viscous dispersions, and nearly quantitative precipitation of the starch-stabilized AgNP was observed at low pH. When compared with a process carried out under similar conditions using a commercial soluble starch as a stabilizer, smaller AgNP and higher conversions of silver nitrate to water-soluble starch-AgNP were obtained when the amylose–sodium palmitate complex was used.

Acknowledgements

We are grateful to Jeanette Little for technical assistance, Gary Grose for X-ray diffraction data, Kim Ascherl for ICP-AES data, and Arthur Thompson for SEM. TEM was carried out in the Frederick Seitz Materials Research Laboratory Central Facilities, University of Illinois, which are partially supported by the U.S. Department of Energy under Grants DE-FG02-07ER46453 and DE-FG02-07ER46471.

References

Batabyal, S. K., Basu, C., Das, A. R., & Sanyal, G. S. (2007). Green chemical synthesis of silver nanowires and microfibers using starch. *Journal of Biobased Materials and Bioenergy*, *1*, 143–147.

Božanić, D. K., Djoković, V., Blanuša, J., Nair, P. S., Georges, M. K., & Radhakrishnan, T. (2007). Preparation and properties of nano-sized Ag and Ag_2S particles in biopolymer matrix. *European Physical Journal E*, *22*, 51–59.

Božanić, D. K., Djoković, V., Dimitrijević-Branković, S., Krsmanović, R., McPherson, M., Nair, P. S., et al. (2011). Inhibition of microbial growth by silver-starch nanocomposite thin films. *Journal of Biomaterials Science, Polymer Edition*, *22*, 2343–2355.

Bromberg, L., Chen, L., Chang, E. P., Wang, S., & Hatton, T. A. (2010). Reactive silver and cobalt nanoparticles modified with fatty acid ligands functionalized by imidazole derivatives. *Chemistry of Materials*, *22*, 5383–5391.

Byars, J. A., Fanta, G. F., Kenar, J. A., & Felker, F. C. (2012). Influence of pH and temperature on the rheological properties of aqueous dispersions of starch–sodium palmitate complexes. *Carbohydrate Polymers*, *88*, 91–95.

Eid, M. (2011). Gamma radiation synthesis and characterization of starch based polyelectrolyte loaded silver nanoparticles. *Journal of Inorganic and Organometallic Polymers and Materials*, *21*, 297–305.

El-Rafie, M. H., El-Naggar, M. E., Ramadan, M. A., Fouda, M. M. G., Al-Deyab, S. S., & Hebish, A. (2011). Environmental synthesis of silver nanoparticles using hydroxypropyl starch and their characterization. *Carbohydrate Polymers*, *86*, 630–635.

Fanta, G. F., Kenar, J. A., Byars, J. A., Felker, F. C., & Shogren, R. L. (2010). Properties of aqueous dispersions of amylose–sodium palmitate complexes prepared by steam jet cooking. *Carbohydrate Polymers*, *81*, 645–651.

Gao, X., Wei, L., Yan, H., & Xu, B. (2011). Green synthesis and characteristic of core-shell structure silver/starch nanoparticles. *Materials Letters*, *65*, 2963–2965.

Ghaseminezhad, S. M., Hamedi, S., & Shojaosadati, S. A. (2012). Green synthesis of silver nanoparticles by a novel method: Comparative study of their properties. *Carbohydrate Polymers*, *89*, 467–472.

Hebeish, A., El-Naggar, M. E., Fouda, M. M. G., Ramadan, M. A., Al-Deyab, S. S., & El-Rafie, M. H. (2011). Highly effective antibacterial textiles containing green synthesized silver nanoparticles. *Carbohydrate Polymers*, *86*, 936–940.

Hu, B., Wang, S.-B., Wang, K., Zhang, M., & Yu, S.-H. (2008). Microwave-assisted rapid facile "green" synthesis of uniform silver nanoparticles: Self assembly into

multilayered films and their optical properties. *Journal of Physical Chemistry C*, *112*, 11169–11174.

Islam, M. R. (2010). Household microwave-mediated carbohydrate-based production of silver nanomaterials. US Patent No. 8,062,407, Issue date: November 22, 2011.

Johnston, D. A., Mukerjea, R., & Robyt, J. F. (2011). Preparation and characterization of new and improved soluble-starches, -amylose, and -amylopectin by reaction with benzaldehyde/zinc chloride. *Carbohydrate Research*, *346*, 2777–2784.

Kakkar, R., Sherly, E. D., Madgula, K., Devi, D. K., & Sreedhar, B. (2012). Synergetic effect of sodium citrate and starch in the synthesis of silver nanoparticles. *Journal of Applied Polymer Science*, *126*, E154–E161.

Kassaee, M. Z., Akhavan, A., Sheikh, N., & Beteshobabrud, R. (2008). γ-Ray synthesis of starch-stabilized silver nanoparticles with antibacterial activities. *Radiation Physics and Chemistry*, *77*, 1074–1078.

Klem, R. E., & Brogley, D. A. (1981). Methods for selecting the optimum starch binder preparation system. *Pulp & Paper*, *55*, 98–103.

Konwarh, R., Karak, N., Sawian, C. E., Baruah, S., & Mandal, M. (2011). Effect of sonication and aging on the templeting attribute of starch for "green" silver nanoparticles and their interactions at bio-interface. *Carbohydrate Polymers*, *83*, 1245–1252.

Lintner, C. J. J. (1886). Studien über diastase. *Journal für Praktische Chemie*, *34*, 378–394.

Luo, S. Y., Chen, J., Chen, M., Xu, W. C., & Zhang, X. L. (2012). Antibacterial activity of silver nanoparticles colloidal sol and its application in package film. *Advanced Materials Research*, *380*, 254–259.

Ma, W.-P., & Robyt, J. F. (1987). Preparation and characterization of soluble starches having different molecular sizes and composition, by acid hydrolysis in different alcohols. *Carbohydrate Research*, *166*, 283–297.

Marie Arockianathan, P., Sekar, S., Kumaran, B., & Sastry, T. P. (2012). Preparation, characterization and evaluation of biocomposite films containing chitosan and sago starch impregnated with silver nanoparticles. *International Journal of Biological Macromolecules*, *50*, 939–946.

Morones, J. R., Elechiguerra, J. L., Camacho, A., Holt, K., Kouri, J. B., Ramirez, J. T., et al. (2005). The bactericidal effect of silver nanoparticles. *Nanotechnology*, *16*, 2346–2353.

Raveendran, P., Fu, J., & Wallen, S. L. (2003). Completely "green" synthesis and stabilization of metal nanoparticles. *Journal of the American Chemical Society*, *125*, 13940–13941.

Raveendran, P., Fu, J., & Wallen, S. L. (2006). A simple and "green" method for the synthesis of Au, Ag, and Au-Ag alloy nanoparticles. *Green Chemistry*, *8*, 34–38.

Sharma, V. K., Yngard, R. A., & Lin, Y. (2009). Silver nanoparticles: Green synthesis and their antimicrobial activities. *Advances in Colloid and Interface Science*, *145*, 83–96.

Shervani, Z., & Yamamoto, Y. (2011). Carbohydrate-directed synthesis of silver and gold nanoparticles: Effect of the structure of carbohydrates and reducing agents on the size and morphology of the composites. *Carbohydrate Research*, *346*, 651–658.

Valodkar, M., Bhadoria, A., Pohnerkar, J., Mohan, M., & Thakore, S. (2010). Morphology and antibacterial activity of carbohydrate-stabilized silver nanoparticles. *Carbohydrate Research*, *345*, 1767–1773.

Valodkar, M., Modi, S., Pal, A., & Thakore, S. (2011). Synthesis and anti-bacterial activity of Cu, Ag and Cu–Ag alloy nanoparticles: A green approach. *Materials Research Bulletin*, *46*, 384–389.

Vigneshwaran, N., Nachane, R. P., Balasubramanya, R. H., & Varadarajan, P. V. (2006). A novel one-pot "green" synthesis of stable silver nanoparticles using soluble starch. *Carbohydrate Research*, *341*, 2012–2018.

Vimala, K., Sivudu, K. S., Mohan, Y. M., Sreedhar, B., & Raju, K. M. (2009). Controlled silver nanoparticles synthesis in semi-hydrogel networks of poly(acrylamide) and carbohydrates: A rational methodology for antibacterial application. *Carbohydrate Polymers*, *75*, 463–471.

White, R. J., Budarin, V. L., Moir, J. W. B., & Clark, J. H. (2011). A sweet killer: Mesoporous polysaccharide confined silver nanoparticles for antibacterial applications. *International Journal of Molecular Sciences*, *12*, 5782–5796.